Chemistry Publications   Chemistry Department

2017

Do fractionally incremented nuclear charges improve time-dependent density functional theory excitation energies as reliably as fractional orbital populations?

Darya N. Komsa

Viktor N. Staroverov

Do fractionally incremented nuclear charges improve time-dependent density-functional-theory excitation energies as reliably as fractional orbital populations?

Darya N. Komsa[1] · **Viktor N. Staroverov**[1]

Abstract Gaiduk *et al.* (2012) [Phys Rev Lett 108:253005] showed that one can improve local, semilocal, and hybrid approximations to the Kohn–Sham effective potentials of atoms and molecules by removing a system-independent fraction of electron charge from the highest-occupied molecular orbital (HOMO); if the corrected Kohn–Sham potential is used for adiabatic linear-response time-dependent density-functional theory (TDDFT) calculations, accurate Rydberg excitation energies are obtained. One may ask whether the same effect could also be achieved by fractionally increasing the positive charges of the nuclei. We investigate this question and find that a small increase of nuclear charges can indeed substantially reduce errors in TDDFT Rydberg excitation energies. However, the optimal magnitude of the charge increase is system-dependent. In addition, the procedure is ambiguous for molecules, where one has to decide how to distribute the additional charge among individual nuclei. These two drawbacks of the fractional nuclear charge method make it disadvantageous compared to the HOMO depopulation technique.

Keywords Excited states · TDDFT · Fractional occupations · Effective nuclear charge · Model exchange-correlation potentials

1 Introduction

Adiabatic time-dependent density-functional theory (TDDFT) in the linear-response regime [1–3] is a common method for calculating vertical electronic excitation energies. TDDFT with traditional (local, semilocal, and hybrid) density-functional approximations gives a reasonable accuracy of roughly 0.2 eV for valence excitations but significantly (by 1 eV or

Corresponding author: Viktor N. Staroverov
Tel.: +1-519-661-2111 ext 86317
Fax: +1-519-661-3022
E-mail: vstarove@uwo.ca

[1]Department of Chemistry, The University of Western Ontario, London, Ontario N6A 5B7, Canada

more) underestimates Rydberg excitation energies [4–7]. This happens because exchange-correlation potentials derived from traditional density functionals are not negative enough and decay too fast with increasing distance from the nuclei [2, 3, 8]. TDDFT description of Rydberg excitations can be improved by switching from traditional to range-separated hybrid functionals [9–12] or to directly approximated exchange-correlation potentials [13–17]. It is also possible to obtain accurate Rydberg excitations by combining traditional functionals with shape corrections [15, 18–20], quantum defect theory [21], the highest-occupied molecular orbital (HOMO) depopulation method [22–24], and other techniques [25–29].

In the HOMO depopulation method [22, 23], the corrected Kohn–Sham potential of a finite system is obtained by performing a self-consistent-field (SCF) calculation on an auxiliary system in which the HOMO occupation number is reduced by δ ($0 \leq \delta \leq 1$). The optimal value of δ turns out to be almost system-independent but varies from one functional to another. When the Kohn–Sham orbitals and orbital eigenvalues computed with the corrected Kohn–Sham potential are substituted, in a post-SCF fashion, into the Casida equations [1] for the corresponding *neutral* system of interest, the mean absolute error (MAE) in predicted Rydberg excitation energies decreases by almost an order of magnitude, while the accuracy for valence transition is barely affected [22, 23]. The optimal values of δ cluster around 0.25 for local and semilocal density-functional approximations, and are in the neighborhood of 0.17 for hybrid functionals [22].

The HOMO depopulation method can be applied to any approximate density functional, has no added computational cost, and is easy to implement. In an independent study, Li and Truhlar [24] found that, for a test set of 69 excited states (both valence and Rydberg) of 11 closed-shell organic molecules, the HOMO-depopulation TDDFT technique with common semilocal and hybrid density functionals outperforms even the equation-of-motion coupled cluster singles and doubles method [30], a highly accurate but computationally demanding *ab initio* technique.

Loosely speaking, the HOMO depopulation method works by making an approximate Kohn–Sham potential more attractive in the valence and asymptotic regions. One may therefore wonder whether the same beneficial effect on the shape of $v_{\mathrm{HXC}}(\mathbf{r})$ could be achieved in an even simpler manner—by leaving the orbital occupation numbers unchanged but increasing the nuclear charge(s) instead. In this work we answer that question.

2 Methodology

In the Kohn–Sham density functional theory [31], the electron density of a spin-compensated N-electron system is given by $\rho(\mathbf{r}) = 2\sum_{i=1}^{N/2}|\phi_i(\mathbf{r})|^2$, where $\phi_i(\mathbf{r})$ are the lowest-eigenvalue self-consistent solutions of the equation

$$\left[-\frac{1}{2}\nabla^2 + v_{\mathrm{eff}}(\mathbf{r})\right]\phi_i(\mathbf{r}) = \varepsilon_i\phi_i(\mathbf{r}), \tag{1}$$

with

$$v_{\mathrm{eff}}(\mathbf{r}) = v(\mathbf{r}) + v_{\mathrm{HXC}}([\rho];\mathbf{r}). \tag{2}$$

Here $v(\mathbf{r})$ is the external potential of the nuclei and $v_{\mathrm{HXC}}([\rho];\mathbf{r})$ is the density-dependent Hartree–exchange-correlation potential. The latter is in turn decomposed as

$$v_{\mathrm{HXC}}([\rho];\mathbf{r}) = v_{\mathrm{H}}([\rho];\mathbf{r}) + v_{\mathrm{XC}}([\rho];\mathbf{r}), \tag{3}$$

where $v_H([\rho];\mathbf{r}) = \int \rho(\mathbf{r}')|\mathbf{r}-\mathbf{r}'|^{-1} d\mathbf{r}'$ is the electrostatic (Hartree) potential of $\rho(\mathbf{r})$ and $v_{XC}([\rho];\mathbf{r})$ is the exchange-correlation potential which represents the remainder of electron-electron interactions.

In the HOMO depopulation method [22, 23], one corrects the approximate Kohn–Sham potential of an N-electron system of interest by replacing $v_{HXC}([\rho];\mathbf{r})$ with $v_{HXC}([\rho_\delta];\mathbf{r})$, where $\rho_\delta(\mathbf{r})$ is the self-consistent electron density obtained by removing a fraction δ ($0 \leq \delta \leq 1$) of electron from the HOMO level. For spin-compensated systems with m degenerate spatial HOMOs, the scheme requires removing $\delta/2m$ spin-up and $\delta/2m$ spin-down electrons from each degenerate orbital [22]. Obviously, the density of the fractionally ionized system is such that

$$\int \rho_\delta(\mathbf{r}) d\mathbf{r} = N - \delta. \tag{4}$$

Consider now a different way of introducing the fractional positive charge into a finite system. Let ζ ($0 \leq \zeta \leq 1$) be the total positive charge added to all of the nuclei of the system. For an atom of an element with atomic number Z, this means increasing the nuclear charge from Z to $Z + \zeta$. For a molecule, we distribute the total additional charge among all of the nuclei with weights proportional to their atomic numbers, that is, by changing each Z_A to $Z_A + \zeta_A$, where

$$\zeta_A = \frac{Z_A}{\sum_B Z_B} \zeta. \tag{5}$$

Other ways of partitioning ζ among the nuclei are certainly possible (e.g., based on the density of the HOMO, the average local ionization energy [32–35], the difference between the total electron densities of the cation and the neutral system) but they are not the subject of this work.

The external potential $v_\zeta(\mathbf{r})$ of this auxiliary system is now more negative, i.e., $v_\zeta(\mathbf{r}) < v(\mathbf{r})$. The corresponding density $\rho_\zeta(\mathbf{r})$ increases relative to $\rho(\mathbf{r})$ in the atomic core regions but decreases elsewhere and is such that

$$\int \rho_\zeta(\mathbf{r}) d\mathbf{r} = \int \rho(\mathbf{r}) d\mathbf{r} = N. \tag{6}$$

As a result, the exchange-correlation potential in the valence and asymptotic regions of the auxiliary system will be less negative than in the initial system. However, the Hartree potential as a function of the density varies faster at a given $\mathbf{r}$ than $v_{XC}(\mathbf{r})$, so the net result of increasing the nuclear charges is that $v_{HXC}([\rho_\zeta];\mathbf{r})] < v_{HXC}([\rho];\mathbf{r})]$ in the valence and asymptotic regions, as in the fractional HOMO depopulation method. Of course, $v_{HXC}([\rho_\zeta];\mathbf{r})]$ for some ζ is different from $v_{HXC}([\rho_\delta];\mathbf{r})]$ for $\delta = \zeta$, and it remains to be seen which correction scheme performs better.

The idea is to compute the total Kohn–Sham effective potential of the auxiliary (fractionally charged) system and use it as an improved approximation to the total Kohn–Sham effective potential of the neutral system. The above manipulations with nuclear charges amount to replacing $v_{eff}(\mathbf{r})$ with

$$\tilde{v}_{eff}(\mathbf{r}) = v_\zeta(\mathbf{r}) + v_H([\rho_\zeta];\mathbf{r}) + v_{XC}([\rho_\zeta];\mathbf{r}). \tag{7}$$

Equation (7) may also be written as

$$\tilde{v}_{eff}(\mathbf{r}) = v(\mathbf{r}) + v_H([\rho];\mathbf{r}) + v_{XC}^{corrected}(\mathbf{r}), \tag{8}$$
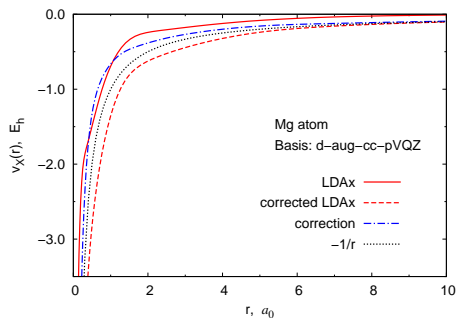
Fig. 1 Exchange-only LDA potentials for the Mg atom before and after applying the nuclear charge correction. The corrected potential is obtained by Eq. (9) using $\zeta = 1$, a larger-than-optimal value chosen for illustrative purposes

where

$$
\begin{aligned}
v_{\mathrm{XC}}^{\mathrm{corrected}}(\mathbf{r}) = {} & v_\zeta(\mathbf{r}) - v(\mathbf{r}) + v_{\mathrm{H}}([\rho_\zeta]; \mathbf{r}) - v_{\mathrm{H}}([\rho]; \mathbf{r}) \\
& + v_{\mathrm{XC}}([\rho_\zeta]; \mathbf{r}).
\end{aligned} \tag{9}
$$

Thus, modification of nuclear charges may be interpreted as a replacement of the exchange-correlation part of $v_{\mathrm{eff}}(\mathbf{r})$ with a *model* exchange-correlation potential formally defined by Eq. (9). Manipulations with nuclear charges are then nothing more than a recipe for constructing a model exchange-correlation potential for the neutral system of interest.

The model exchange-correlation potential of Eq. (9) is more attractive in the valence and asymptotic regions and decays as $-\zeta/r$ at large r, which is closer to the correct $-1/r$ behavior than the exponential or $-1/r^\alpha$ ($\alpha > 1$) decay of traditional local and semilocal approximations [36]. Figure 1 illustrates this result for the exchange-only local density approximation (LDA) for the Mg atom. Although the behavior of each curve at $r = 0$ is not seen in Fig. 1, the original LDA potential is finite at the nucleus, whereas $v_{\mathrm{XC}}^{\mathrm{corrected}}(\mathbf{r})$ tends to $-\infty$ as $r \to 0$. The singularity arises from the external potential difference $v_\zeta(\mathbf{r}) - v(\mathbf{r})$ in Eq. (9). It does not cause any problems, however, because most exchange-correlation potentials of the generalized gradient approximation (GGA) type already have a singularity at each nucleus [37].

Now let us compare the performance of the fractional nuclear charge method to that of the HOMO depopulation technique.

3 Computational details

All calculations reported in this work were performed with the *Gaussian 09* program [38] using the d-aug-cc-pVQZ basis set for atoms and d-aug-cc-pVTZ for molecules. These basis sets were constructed by augmenting the standard aug-cc-pVQZ and aug-cc-pVTZ basis sets with one additional set of diffuse functions as explained in the Supplementary Material.

The HOMO depopulation and fractional nuclear charge schemes are two-step procedures. In the first step, a particular density-functional approximation is used to obtain the SCF solution of the Kohn–Sham equations for a fractionally charged system. In the second step, the Kohn–Sham orbitals and orbital eigenvalues from the first step are used, in a post-SCF fashion, to construct and solve Casida's equations for the neutral system of interest
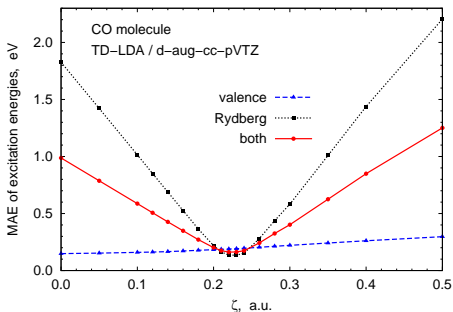
Fig. 2 Determination of the optimal ζ value for the LDA exchange-correlation functional. The plots show the MAEs for the 7 valence, 7 Rydberg, and all 14 TDLDA excitation energies of the CO molecule as a function of ζ. The smallest MAEs are obtained for $\zeta = 0.22$

(i.e., for the same molecular geometry). In both schemes, all linear-response TDDFT coupling matrix elements are computed with the same approximate density functional that was used in the first step.

The test set used in this work was the same as in Ref. [22]. This set, referred to as E-104 here, includes electronic excitation energies of three atoms (Be, Mg, Zn) and six molecules (CO, CH_2O, C_2H_2, C_2H_4, H_2O, N_2) at their experimental geometries. The total numbers of electronic transitions in this test set is 104, including 31 valence and 73 Rydberg excitations. The following representative density-functional approximations were tested: the LDA with the Perdew–Wang parametrization for correlation [39], the Becke–Lee–Yang–Parr (BLYP) GGA [40, 41], the Becke three-parameter hybrid functional with the Lee–Yang–Parr correlation (B3LYP) [42] and the Tao–Perdew–Staroverov–Scuseria (TPSS) meta-GGA [43].

By analogy with the HOMO depopulation procedure of Ref. [22], the optimal value of ζ for each functional was determined by fitting 14 (7 valence and 7 Rydberg) calculated excitation energies of the CO molecule to the corresponding experimental values. The resulting $\zeta = \zeta_{CO}$ value was then used without any adjustments for calculations with the same functional on all other atoms and molecules. For the LDA, the fitting procedure is illustrated by Fig. 2. The optimal ζ values for other density functionals were determined similarly. The results are: $\zeta_{CO} = 0.22$ for LDA, $\zeta_{CO} = 0.26$ for BLYP, $\zeta_{CO} = 0.14$ for B3LYP, and $\zeta_{CO} = 0.20$ for TPSS.

4 Results

The MAEs of the E-104 electronic excitation energies calculated using various methods and approximate density functionals are collected in Table 1. According to this Table, the fractional nuclear charge method always reduces the MAE in calculated Rydberg excitation energies, but not very consistently, and sometimes worsens the functional's performance for valence excitations. Clearly, whereas the fractional HOMO depopulation works equally well for both atoms and molecules, the fractional nuclear charge technique with ζ values optimized for the CO molecule gives relatively poor results for atoms. This makes the overall performance of the fractional nuclear charge much less impressive than the performance of the HOMO depopulation scheme.

To find out whether the relatively poor performance of the fractional nuclear charge method for atoms is due to the use of ζ_{CO} values favoring molecules, we refitted all functional-

Table 1 MAEs (in eV) relative to experiment for the E-104 vertical excitation energies calculated using TDDFT with and without shape corrections for Kohn–Sham potentials. The optimal values of parameters δ and $\zeta = \zeta_{CO}$ for each functional are shown in parentheses

	Atoms			Molecules			Atoms and molecules		
Functional	Valence	Rydberg	All	Valence	Rydberg	All	Valence	Rydberg	All
Uncorrected[a]									
LDA	0.22	0.98	0.81	0.27	1.39	1.02	0.26	1.27	0.97
BLYP	0.29	1.26	1.05	0.35	1.77	1.30	0.34	1.61	1.24
B3LYP	0.29	0.94	0.80	0.36	0.98	0.78	0.35	0.97	0.78
TPSS	0.49	1.10	0.97	0.31	1.45	1.08	0.35	1.35	1.05
Corrected by the HOMO depopulation method[a]									
LDA ($\delta = 0.24$)	0.29	0.23	0.25	0.22	0.25	0.24	0.23	0.24	0.24
BLYP ($\delta = 0.28$)	0.32	0.19	0.22	0.26	0.18	0.21	0.28	0.18	0.21
B3LYP ($\delta = 0.18$)	0.24	0.29	0.28	0.38	0.15	0.23	0.36	0.19	0.24
TPSS ($\delta = 0.23$)	0.35	0.22	0.25	0.29	0.18	0.22	0.30	0.19	0.22
Corrected by the fractional nuclear charge method									
LDA ($\zeta = 0.22$)	0.48	0.58	0.56	0.24	0.22	0.23	0.29	0.33	0.32
BLYP ($\zeta = 0.26$)	0.56	0.60	0.59	0.25	0.16	0.19	0.31	0.29	0.30
B3LYP ($\zeta = 0.14$)	0.24	0.21	0.22	0.33	0.17	0.22	0.31	0.18	0.22
TPSS ($\zeta = 0.20$)	0.42	0.40	0.41	0.31	0.18	0.23	0.33	0.25	0.27

[a]Last-digit discrepancies with Ref. [22] are caused by the fact that Ref. [22] used different exponents for the additional d and f diffuse functions of the Mg atom (see the Supplementary Material).
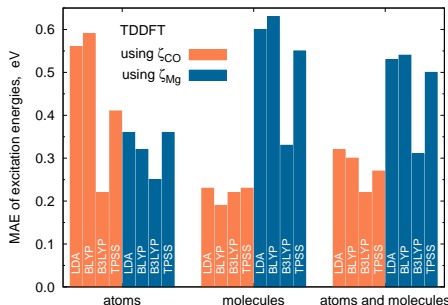
Fig. 3 MAEs of the electronic excitation energies of the E-104 test set calculated using two different ζ values for each functional: one fitted to the 14 experimental excitation energies of the CO molecule, the other fitted to the 8 experimental excitation energies of the Mg atom. The ζ_{CO} values give good results for molecules but not for atoms. The ζ_{Mg} values give good results for atoms but not for molecules

specific ζ values by minimizing the MAE of the 8 (2 valence and 6 Rydberg) excitation energies of the Mg atom. This gave $\zeta_{Mg} = 0.09$ for LDA, $\zeta_{Mg} = 0.14$ for BLYP, $\zeta_{Mg} = 0.10$ for B3LYP, and $\zeta_{Mg} = 0.11$ for TPSS (see the Supplementary Material). Although the refitted parameters did lower the combined (valence and Rydberg) excitation-energy MAEs for the atoms to 0.36 eV (LDA), 0.32 eV (BLYP), 0.25 eV (B3LYP), and 0.36 eV (TPSS), the combined (valence and Rydberg) MAEs for the molecules increased to 0.60 eV (LDA), 0.63 eV (BLYP), 0.33 eV (B3LYP), and 0.55 eV (TPSS). The overall performance of the scheme with ζ_{Mg} values was worse than with ζ_{CO} values for all functionals (Fig. 3). This shows that the fractional nuclear charge method lacks the key feature of the fractional HOMO depopulation technique—transferability of the optimal charge increase value from one system to another.

Another concern about the fractional nuclear charge method is that contracted basis sets such as d-aug-cc-pVQZ may be deficient for atoms and molecules with incremented

nuclear charges. As a result, TDDFT description of core orbitals and, indirectly, electronic excitation energies may be adversely affected by having suboptimal basis-set exponents and contraction coefficients when $\zeta > 0$. To assess the extent of this problem, we computed and compared all of the atomic excitation energies of the E-104 test set for a series of ζ values using two basis sets: the contracted d-aug-cc-pVQZ and the fully uncontracted d-aug-cc-pVQZ (denoted "u-d-aug-cc-pVQZ"). The latter has sufficiently tight primitive basis functions to accommodate higher than normal nuclear charges. For each atom and each ζ value, we evaluated the mean absolute deviation (MAD) in the calculated excitation energies caused by the basis-set decontraction,

$$\text{MAD} = \frac{1}{n} \sum_{i=1}^{n} |E_i(\text{uncontracted}) - E_i(\text{contracted})|, \tag{10}$$

where the summation is over all valence and Rydberg excitation energies of the E-104 test set for the corresponding atom. We found that, in the relevant range $0 \leq \zeta \leq 0.3$, decontraction of the basis set usually results in MADs of 0.001–0.03 eV and never exceeds 0.1 eV, the Be atom being the worst case (see Fig. S1 in the Supplementary Material). These deviations are substantially smaller than the average variations of excitation energies caused by changes in ζ alone (Fig. 2), which suggests that reoptimization of ζ values using more flexible basis sets would not have affected the results significantly.

5 Conclusion

We have investigated the fractional nuclear charge method for TDDFT calculations of Rydberg electronic excitation energies as a possible alternative to the fractional HOMO depopulation technique of Ref. [22]. The accuracy of these two schemes is controlled by functional-specific values of parameters ζ (additional nuclear charge) and δ (HOMO level depopulation), respectively. From calculations on the E-104 test set of valence and Rydberg excitation energies it appears that the parameter ζ of the fractional nuclear charge method exhibits considerable system-dependence, unlike the parameter δ of the HOMO depopulation scheme. For a given density-functional approximation, the ζ value that is optimal for atoms is suboptimal for molecules, and *vice versa*. As a consequence, the fractional nuclear charge method performs less accurately overall than the fractional HOMO depopulation technique. Another disadvantage of the fractional nuclear charge method is that it is ambiguous for molecules, that is, it requires deciding how to distribute the total additional nuclear charge ζ among the nuclei. For these reasons, we conclude that the fractional nuclear charge method is not a viable alternative to the HOMO depopulation technique.

References

1. Casida ME (1995) Time-dependent density functional response theory for molecules. In: Chong DP (ed) Recent Advances in Density Functional Methods, Part I, World Scientific, Singapore, pp 155–192
2. Elliott P, Furche F, Burke K (2009) Excited states from time-dependent density functional theory. Rev Comput Chem 26:91–165

3. Casida ME, Huix-Rotllant M (2012) Progress in time-dependent density-functional theory. Annu Rev Phys Chem 63:287–323
4. Casida ME, Jamorski C, Casida KC, Salahub DR (1998) Molecular excitation energies to high-lying bound states from time-dependent density-functional response theory: Characterization and correction of the time-dependent local density approximation ionization threshold. J Chem Phys 108:4439–4449
5. Caricato M, Trucks GW, Frisch MJ, Wiberg KB (2012) Electronic transition energies: A study of the performance of a large range of single reference density functional and wave function methods on valence and Rydberg states compared to experiment. J Chem Theory Comput 6:370–383
6. Leang SS, Zahariev F, Gordon MS (2012) Benchmarking the performance of time-dependent density functional methods. J Chem Phys 136:104101
7. Isegawa M, Peverati R, Truhlar DG (2012) Performance of recent and high-performance approximate density functionals for time-dependent density functional theory calculations of valence and Rydberg electronic transition energies. J Chem Phys 137:244104
8. Gritsenko OV, Mentel ŁM, Baerends EJ (2016) On the errors of local density (LDA) and generalized gradient (GGA) approximations to the Kohn–Sham potential and orbital energies. J Chem Phys 144:204114
9. Iikura H, Tsuneda T, Yanai T, Hirao K (2001) A long-range correction scheme for generalized-gradient-approximation exchange functionals. J Chem Phys 115:3540–3544
10. Yanai T, Tew DP, Handy NC (2004) A new hybrid exchange-correlation functional using the Coulomb-attenuating method (CAM-B3LYP). Chem Phys Lett 393:51–57
11. Vydrov OA, Scuseria GE (2006) Assessment of a long-range corrected hybrid functional. J Chem Phys 125:234109
12. Chai JD, Head-Gordon M (2008) Long-range corrected hybrid density functionals with damped atom-atom dispersion corrections. Phys Chem Chem Phys 10:6615–6620
13. van Leeuwen R, Baerends EJ (1994) Self-consistent approximation to the Kohn–Sham exchange potentials. Phys Rev A 49:2421–2431
14. Schipper PRT, Gritsenko OV, van Gisbergen SJA, Baerends EJ (2000) Molecular calculations of excitation energies and (hyper)polarizabilities with a statistical average of orbital model exchange-correlation potentials. J Chem Phys 112:1344–1352
15. Grüning M, Gritsenko OV, van Gisbergen SJA, Baerends EJ (2001) Shape corrections to exchange-correlation potentials by gradient-regulated seamless connection of model potentials for inner and outer region. J Chem Phys 114:652–660
16. van Meer R, Gritsenko OV, Baerends EJ (2014) Physical meaning of virtual Kohn–Sham orbitals and orbital energies: An ideal basis for the description of molecular excitations. J Chem Theory Comput 10:4432–4441
17. Karolewski A, Armiento R, Kümmel S (2013) Electronic excitations and the Becke–Johnson potential: The need for and the problem of transforming model potentials to functional derivatives. Phys Rev A 88:052519
18. Casida ME, Salahub DR (2000) Asymptotic correction approach to improving approximate exchange-correlation potentials: Time-dependent density-functional theory calculations of molecular excitation spectra. J Chem Phys 113:8918–8935
19. Tozer DJ, Handy NC (1998) Improving virtual Kohn–Sham orbitals and eigenvalues: Application to excitation energies and static polarizabilities. J Chem Phys 109:10180–10189
20. Allen M, Tozer DJ (2000) Kohn–Sham calculations using hybrid exchange-correlation functionals with asymptotically corrected potentials. J Chem Phys 113:5185–5192

21. Wasserman A, Maitra NT, Burke K (2003) Accurate Rydberg excitations from the local density approximation. Phys Rev Lett 91:263001
22. Gaiduk AP, Firaha DS, Staroverov VN (2012) Improved electronic excitation energies from shape-corrected semilocal Kohn–Sham potentials. Phys Rev Lett 108:253005
23. Gaiduk AP, Mizzi D, Staroverov VN (2012) Self-interaction correction scheme for approximate Kohn–Sham potentials. Phys Rev A 86:052518
24. Li SL, Truhlar DG (2014) Testing time-dependent density functional theory with depopulated molecular orbitals for predicting electronic excitation energies of valence, Rydberg, and charge-transfer states and potential energies near a conical intersection. J Chem Phys 141:104106
25. Li SL, Truhlar DG (2015) Improving Rydberg excitations within time-dependent density functional theory with generalized gradient approximations: The exchange-enhancement-for-large-gradient scheme. J Chem Theory Comput 11:3123–3130
26. Seidu I, Krykunov M, Ziegler T (2015) Applications of time-dependent and time-independent density functional theory to Rydberg transitions. J Phys Chem A 119:5107–5116
27. Nakata A, Imamura Y, Nakai H (2006) Hybrid exchange-correlation functional for core, valence, and Rydberg excitations: Core-valence-Rydberg B3LYP. J Chem Phys 125:064109
28. Gudmundsdóttir H, Zhang Y, Weber PM, Jónsson H (2013) Self-interaction corrected density functional calculations of molecular Rydberg states. J Chem Phys 139:194102
29. van Faassen M, Burke K (2009) Time-dependent density functional theory of high excitations: To infinity and beyond. Phys Chem Chem Phys 11:4437–4450
30. Stanton JF, Bartlett RJ (1993) The equation of motion coupled-cluster method. A systematic biorthogonal approach to molecular excitation energies, transition probabilities, and excited state properties. J Chem Phys 98:7029–7039
31. Kohn W, Sham LJ (1965) Self-consistent equations including exchange and correlation effects. Phys Rev 140:A1133–A1138
32. Sjoberg P, Murray JS, Brinck T, Politzer P (1990) Average local ionization energies on the molecular surfaces of aromatic systems as guides to chemical reactivity. Can J Chem 68:1440–1443
33. Politzer P, Murray JS, Bulat FA (2010) Average local ionization energy: A review. J Mol Model 16:1731–1742
34. Ryabinkin IG, Staroverov VN (2014) Average local ionization energy generalized to correlated wavefunctions. J Chem Phys 141:084107
35. Kohut SV, Cuevas-Saavedra R, Staroverov VN (2016) Generalized average local ionization energy and its representations in terms of Dyson and energy orbitals. J Chem Phys 145:074113
36. Engel E, Chevary JA, Macdonald LD, Vosko SH (1992) Asymptotic properties of the exchange energy density and the exchange potential of finite systems: Relevance for generalized gradient approximations. Z Phys D 23:7–14
37. Umrigar CJ, Gonze X (1994) Accurate exchange-correlation potentials and total-energy components for the helium isoelectronic series. Phys Rev A 50:3827–3837
38. Frisch MJ, Trucks GW, Schlegel HB, Scuseria GE, Robb MA, Cheeseman JR, Scalmani G, Barone V, Mennucci B, Petersson GA, Nakatsuji H, Caricato M, Li X, Hratchian HP, Izmaylov AF, Bloino J, Zheng G, Sonnenberg JL, Hada M, Ehara M, Toyota K, Fukuda R, Hasegawa J, Ishida M, Nakajima T, Honda Y, Kitao O, Nakai H, Vreven T, Montgomery JrJA, Peralta JE, Ogliaro F, Bearpark M, Heyd JJ, Brothers E, Kudin KN, Staroverov VN, Kobayashi R, Normand J, Raghavachari K, Rendell A, Burant JC,

Iyengar SS, Tomasi J, Cossi M, Rega N, Millam JM, Klene M, Knox JE, Cross JB, Bakken V, Adamo C, Jaramillo J, Gomperts R, Stratmann RE, Yazyev O, Austin AJ, Cammi R, Pomelli C, Ochterski JW, Martin RL, Morokuma K, Zakrzewski VG, Voth GA, Salvador P, Dannenberg JJ, Dapprich S, Daniels AD, Farkas Ö, Foresman JB, Ortiz JV, Cioslowski J, Fox DJ. *Gaussian 09*, Revision B.1, Gaussian Inc., Wallingford, CT (2010)

39. Perdew JP, Wang Y (1992) Accurate and simple analytic representation of the electron-gas correlation energy. Phys Rev B 45:13244–13249

40. Becke AD (1988) Density-functional exchange-energy approximation with correct asymptotic behavior. Phys Rev A 38:3098–3100

41. Lee C, Yang W, Parr RG (1988) Development of the Colle–Salvetti correlation-energy formula into a functional of the electron density. Phys Rev B 37:785–789

42. Stephens PJ, Devlin FJ, Chabalowski CF, Frisch MJ (1994) *Ab initio* calculation of vibrational absorption and circular dichroism spectra using density functional force fields. J Phys Chem 98:11623–11627

43. Tao J, Perdew JP, Staroverov VN, Scuseria GE (2003) Climbing the density functional ladder: Nonempirical meta-generalized gradient approximation designed for molecules and solids. Phys Rev Lett 91:146401